IRAQI Academic Scientific Journals

Samarra Journal of Pure and Applied Science

SJPAS

p ISSN: 2663-7405
e ISSN: 2789-6838

www.sjpas.com

# Green Fabrication of Copper Oxide Nanoparticles from Imperata Cylindrical and Evaluating Anticancer Potential Against Human HCT-116 Cell and Antibacterial Activity

**Mohammed Mahmood Masood*, Wadhah Naji Al Sieadi**
Department of Chemistry, College of Science, University of Baghdad, Iraq



https://doi.org/10.54153/sjpas.2025.v7i1.829

**Article Information**

Received: 10/03/2024
Revised: 20/04/2024
Accepted: 28/05/2024
Published: 30/03/2025

**Keywords:**

*Imperata cylindrical, Copper oxide nanoparticles, Anticancer, HCT-116 and Antibacterial*

**Corresponding Author**

E-mail: Mohammed.mahmoud1105d@sc.uobaghdad.edu.iq
Mobile: +9647736914970

**Abstract**

The present study investigates the in vitro anticancer and antibacterial of copper oxide nanoparticles (CuO NPs) synthesized from *Imperata cylindrica* using MTT Assay (3-(4,5-dimethylthiazol-2-yl)-2,5-diphenyl-2H-tetrazolium bromide) and the well diffusion method. The synthesized CuO NPs nanoparticles were analyzed by several analytical techniques such as UV–visible, Fourier transform infra-red, energy dispersive X-ray analyses with mean size 10.9 nm., Field emission scanning electron micrographs with size distribution ranging from 28.59 to 34.78 nm, Atomic forces microscope with mean diameter 21.02nm and zeta potential analysis. The efficiency of CuO NPs on human colorectal carcinoma cell lines (HCT-116) and HFF as normal cell lines was studied. Different concentrations of copper oxide nanoparticles (10, 50, 100, 250 ,500) µg/ml at 24 hours were selected. Results indicated that the impact of nanoparticles is dependent on the concentration. As the concentration of nanoparticles increases, the percent of cell viability decreases. It was found that concentration of CuO NPs at 250 µg/ml gave the cell viability percent (30.08%) after 24 hours. The nanoparticles also showed antibacterial effects against gram-positive and gram-negative bacteria in different concentrations. At a concentration of 1024 (µg/ml), CuO NPs showed a strong antibacterial effect against all four kinds of bacteria.

## Introduction:

Cancer is one of the contributors to the rise in mortality rate in many countries, and it is also viewed as a dangerous health threat to mankind worldwide, It is the cause of death worldwide, accounting for nearly 10 million deaths in 2020, as per the World Cancer Report from World Health Organization[1].

several side effects when using available cancer treatments like alkylating agents, antimetabolites and other different cancer therapy methods due to the incapability of differentiation between the normal cell and cancer-causing cells, which leads to toxicity [2].

The employing of nanomaterials in cancer treatment has been found in a modern medication due to their nanoscale-sized property, which provide increased drug efficacy and sustained release of drug material[3, 4].

Numerous metallic nanoparticles such as gold, silver, cobalt ,selenium and others have been investigated for their potential anticancer effects [5-9]. However, copper NPs have become increasingly applicable due to their cytotoxic potency against cells of cancer at low doses and high stability period compared to Au and Ag NPs. Moreover, in contrast to gold NPs, they possess a tunable absorption, based on the particle size, which can be formulated below 20 nm, ensuring near-infrared absorption, improved pharmacokinetic properties and efficient elimination from the body when their size is below 6 nm[10].

Copper oxide is a p-type semiconductor used in industries such as gas sensing, solar energy conversion, batteries, magnetic storage media and field emission devices [11]. Biomedical applications of copper oxide nanoparticles involved anti-microbial targeted drug delivery,antifouling, antibiotics and antioxidant [12].

The green synthesis of nanoparticles provides an environmentally friendly, quick, easy, simple, and cost-effective method. You may find an abundance of terpenoids, carbohydrates, phenols, and flavonoids in the plant's many components, including its seeds, flowers, leaves, fruits and stems. These phenolic phytochemicals possess hydroxyl and ketone groups, which may act as stabilizing and reducing agents. Nonetheless, there is still a lot of debate on how plants may be used in green synthesis. [13]

Imperata cylindrica, often called cogon grass, lalang, or halfa in Iraq and the Middle East, a plant species belonging to the Poaceae family. As shown in Figure 1.

**Fig.1** *Imperata cylindrical*

Cogon grass, a highly invasive warm-season perennial grass, is widely recognized as problematic and listed among the most troublesome weeds globally. It adversely affects agriculture and ecosystem health by outcompeting other plants, resulting in stunted growth, decreased crop yields, and delayed harvests. Furthermore, animals refrain from masticating the mature leaves that possess sharp edges.[14] .

However, the existing research on using *Imperata cylindrica* in biological and environmental applications is scarce. This plant was said to possess therapeutic properties.

The medicinal properties of this plant were subsequently validated based on the presence of several phytochemicals such as tannins, alkaloids, saponins, and flavonoids. [15]
Traditionally, some cultures have used this substance in folk treatments to treat cancer, colds, diarrhea, dysentery, gonorrhea, myalgia, night sweats, rheumatism, and tumors.[16].

A limited number of studies that describe the biosynthesis process of nanoparticles from aqueous extract of *Imperata cylindrical*.[17, 18].

The phyto- chemical constituents of plant extract have ability to reducing and capping agent to convert the bulk metallic into nano scale. [19]

The objective of the current research was to biosynthesize CuO nanoparticles from *Imperata cylindrica* for evaluating their effectiveness in inhibiting a human colorectal carcinoma cell line (HCT-116) and Antibacterial Activity.

## EXPERIMENTAL SECTION

### Materials

*Imperata cylindrica* was obtained in December from a village in Diyala Governorate, Iraq. Copper nitrate (99% purity, BHD, Germany), sodium hydroxide(97% purity Sigma-Aldrich,USA), Ethanol 99% purity Sigma-Aldrich,USA),Dimethyl sulphoxide (DMSO) (99% purity Sigma-Aldrich,USA), and sulforhodamine B (SRB) were bought from Sigma-Aldrich. The Dulbecco's Modified Eagle's Medium (DMEM), trypsin-EDTA, penicillin-streptomycin, and fetal bovine serum (FBS) (Welgene, a company, South Korea). The Mito Tracker Red, Hoechst 33252, and 2′, 7′-Dichlorofluorescin diacetate (DCFH-DA) (Santa Cruz Biotechnology, Inc.USA).

### Instrumentation

The characterization of the prepared nanoparticles and detection of cell proliferation in MTT Assay were examined in different techniques as presented in Table (1).

**Table1:** The characterization of CuO NPs and detection of cell proliferation in MTT Assay

| Instrument used | The manufacturer and the model |
|---|---|
| UV–visible spectroscopy | SHEMADZU 2601,Japan |
| Fourier transform infra-red(FTIR) | SHIMADZU 8400S, Japan |
| energy dispersive X-ray analyses(XRD) | XRD, XD-3, persee, China |
| Scanning electron microscopy (SEM) | SEM,tescan -MIRA3, USA |
| Atomic force microscopy (AFM) | Nanosurf AG, Switzerland |
| Zeta potentiometer | Malvern, Zetasizer 7.11, England |
| Cell viability and proliferation measurment in MTT test at a wavelength of 570 nm | Elisa plate reader (Model 50, Bio-Rad Corp, Hercules, California, CA) |

### Procedure

### 2.1. Aqueous Extraction of *Imperata Cylindrica*

The green reducing agents were obtained by collecting the leaves of I. cylindrical in February, which were washed extensively with tap water, followed by distilled water, and left to air dry for one week. The desiccated fragments were pulverized using an electric grinder. A quantity of 5 grams of finely ground powder was introduced into 100 millilitres of distilled water and subjected to heating at a temperature of 70 degrees Celsius for 30 minutes. The extract was cooled and passed through a Whatman filter paper to remove impurities. The

resulting liquid, known as the filtrate, was collected and stored at a temperature of 4 °C for future use[20].

### 2.2. Synthesis of CuO NPs

CuONP nanoparticles were synthesized according to the following method using a technique similar to that reported in earlier works, with some alterations. [21-24]
A 0.10 M Copper(II) nitrate solution was created by dissolving 2.416 g of solid $Cu(NO_3)_2.3H_2O$ in 100 mL of pure water. Following complete dissolution, the solution underwent filtration to eliminate all impurities. The aqueous extract of *Imperata cylindrica* was combined with a solution of 0.10 M $Cu(NO_3)_2.3H_2O$ at a ratio of 4:1 by volume. The mixture was added gently over 15 minutes at room temperature while continuously stirring. The solution underwent a colour transformation following the addition, shifting from a blue colour to a green light. The observed change in colour signifies a reduction in copper nanoparticles. Subsequently, a NaOH (0.1 M) solution was incrementally added until the pH reached 9.0 to 10. The mixture was constantly agitated for 15 minutes while being heated to a temperature of 70°C[25]. The light green copper oxide ($CuOH_2$) exhibited significant precipitation in the beaker, making them readily collectable. The copper particles' precipitate was gathered using centrifugation and promptly washed many times with distilled water and ethanol to eliminate any remaining unreacted particles. The Cu-NPs nanoparticles were subjected to overnight drying and calcination at 350 °C for two hours, developing black precipitate CuO NPs. Subsequently, they were finely crushed into a powder. As shown in Figure (2) .

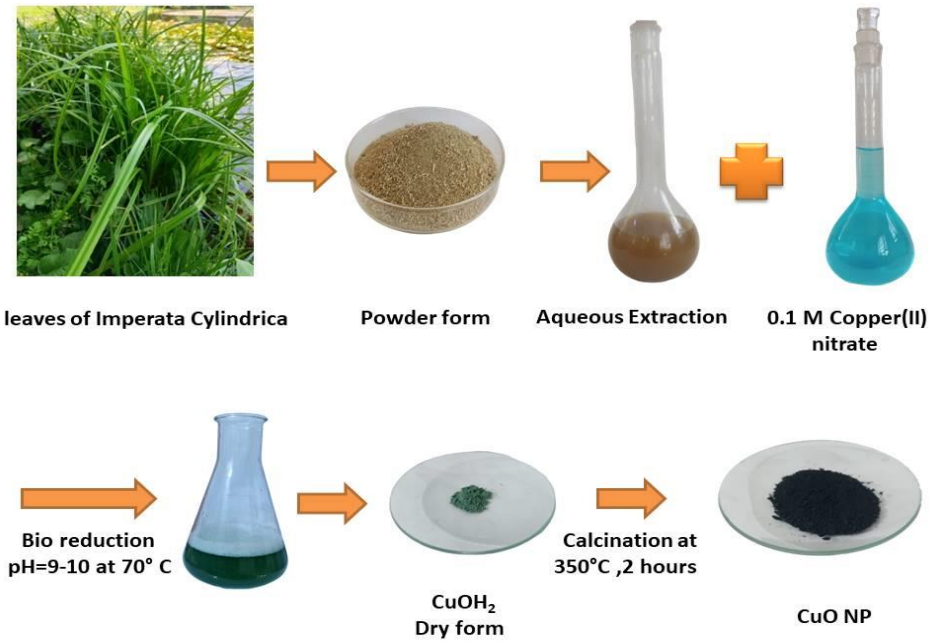


**Fig. 2** *mechanism of green synthesis copper oxide nanoparticle's*

### 2.3. Cell culture of human colon cancer cell lines.

The synthesized compounds were tested for their cytotoxicity against human cancer cells, namely HCT116, using the MTT colourimetric assay. The experiment used culture media as the negative control and cell lines as the positive control. In summary, 104 cells were placed onto a 96-well microplate and kept in a controlled environment with 5% $CO_2$ and 95% air at 37°C until they reached 70-90% confluence.

Before exposing the cells to the particles, the particles were dispersed in cell culture media and subjected to sonication for 10 minutes to create a stock solution with a

concentration of 2 mg/mL. Subsequently, 150 µl of dispersion nanoparticles were introduced into each well to achieve varying concentrations of CuO NPs derived from *Imperata cylindrica* (cogon grass) (10, 50, 100, 250, and 500 µg $mL^{-1}$) correspondingly. The cancer cells were then subjected to this treatment after 24 hours.

The medium was extracted from each well and then rinsed twice for 2-3 minutes with 150 µl of phosphate-buffered saline (PBS). Next, 25 µl of the MTT (3- (4,5 Dimethylthiazole-2-yl)-2,5-diphenyl tetrazolium, Sigma-Aldrich, USA) stock solution was added to each well. The samples were then placed in a humidified environment containing 5% $CO_2$ and 95% air and kept at 37° C for 4 hours. During this phase, the tetrazolium ring is formed by the specific breakdown of mitochondrial dehydrogenases in living cells, producing blue/purple formazan crystals. To facilitate the dissolution of the formazan crystals, 100 µl of dimethyl sulfoxide (DMSO) was given to each well. The solution's optical absorbance (OD) was measured at a wavelength of 570 nm using an Elisa plate reader. The trials were conducted three times each. The cell viability was determined by calculating the percentage of the mean optical density values of each sample relative to the optical density values of the positive control using the formula provided below.[26] equation (1):

$$\text{Viability Percentage} = \frac{(\text{OD sample} - \text{OD blank})}{(\text{OD control} - \text{OD blank})} * 100 \qquad \text{Eq. (1)}$$

where $OD_{sample}$, $OD_{control}$ are the optical density values for experimental cells and control cells , respectively. $OD_{blank}$ is the absorbance of the cell counting kit solution.

### 2.4. Antibacterial activity

The antimicrobial efficacy of copper oxide nanoparticles was assessed against two strains of Gram-negative bacteria (*Pseudomonas aeruginosa* and *Escherichia coli*) and two strains of Gram-positive bacteria (*Staphylococcus* aureus and *Streptococcus*) using the agar healthy diffusion technique[27].

The bacterial isolates were cultivated in nutritional broth and subjected to incubation at a temperature of 37 ºC for 18-24 hours. After incubation, 0.1 ml of each bacterial suspension was evenly distributed over the nutrient agar surface. The agar plates were then kept at 37 ºC for 24 hours. A single colony was introduced into a test tube containing 5 mL of normal saline, resulting in a bacterial suspension with a moderate cloudiness level comparable to the standard turbidity solution, which is approximately equivalent to 1.5x108 CFU/mL. A sterile cotton swab was used to carefully carry a portion of bacterial suspension and evenly distribute it over a Mueller-Hinton agar medium. The media was then kept undisturbed for 10 minutes. The previous agar layer was punctured with wells of five millimetres in diameter (four wells per plate). The agar discs were extracted, and 50µl of Copper Oxide Nanoparticles (CuO NPs) were added. Four concentrations (128, 256, 512, and 1024 µg/ml) were introduced into each well using a micropipette, while the DMSO solvent was added to the centre well as a control. The plates were placed in an incubator at a temperature of 37 ºC for 18 hours. Subsequently, the diameter of the zones of inhibition was measured and recorded.

## 3. RESULTS AND DISCUSSION

### 3.1. Characterization of Cu NPs.

#### 3.1. 1. UV-Visible Analysis of CuO NPs

The research examined the ultraviolet-visible spectra of copper oxide nanoparticles. The UV-Vis spectrum of CuO nanoparticles synthesized by biosynthesis and the UV-Vis spectrum

of the aqueous extract of *Imperata cylindrical* are shown in Figure (3-A). The area of maximum absorbance for copper oxide nanoparticles was around 296.5 nm, mainly owing to surface Plasmon absorption. To ascertain the band gap energy of nano-CuO. The primary absorption, associated with the excitation of electrons from the valence band to the conduction band, may be used to ascertain the optical band gap value.

The provided formula may be used to compute the optical band gap of CuO NPs synthesized in this study based on their UV-Vis spectra.equation (2)[28]:

$$(\alpha h\nu)^{1/d} = A(h\nu - Eg) \qquad \text{Eq. (2)}$$

where α is the absorption coefficient, Eg is the optical band gap, h$\nu$ is the incident photon energy.

The tauc figure in Figure (3-B) illustrates the computation of the direct band gap for CuO NPs, which falls within Eg=3.63 eV. This range exceeds the published value and the band gap of bulk CuO (2.1 eV). The wider band gap in the produced nanoparticles may be attributed to the size-dependent quantum confinement effect. Consequently, the band gap energy increases as the size of particles falls, and the nanocrystals become smaller than the Bohr radius of the excited electron-hole pair.[29].

Consequently, the surface atom exhibits a reduced coordination number and atomic interaction, leading to a rise in the energy of the highest valence band and a reduction in the power of the lowest unoccupied conduction band. As a result, there is an elevation in the bandgap energy. This outcome is consistent with a prior investigation.[30] .

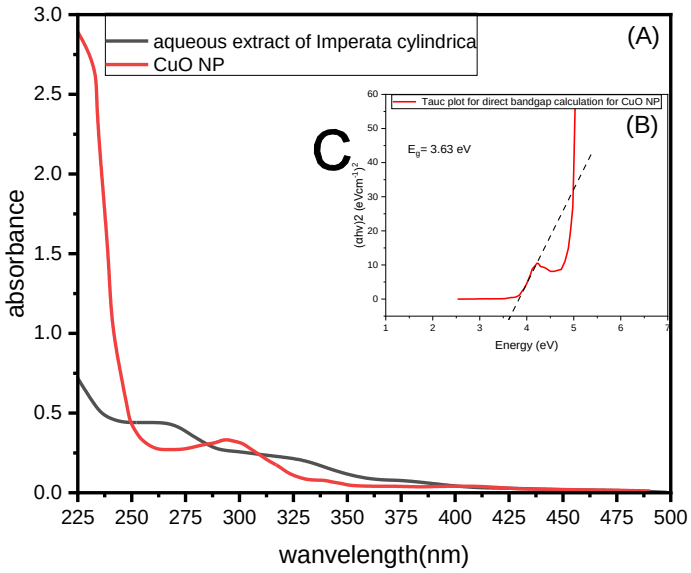


**Fig. 3** *(A) UV-vis spectroscopy of CuO-NPs and aqueous extract of Imperata cylindrical .(B) the Tauc plot for direct band gap calculation for CuO NP*

### 3.1. 2. FTIR Chemical Analysis

FTIR analysis was utilized to determine the functional groups in the produced CuO NPs and compared to the FTIR spectrum of the Aqueous extraction of *Imperata Cylindric*. The Fourier-transform infrared (FTIR) spectra of CuO nanoparticles (NPs) exhibited distinct peaks at certain wavenumbers: 422.41, 493.87, 594.08, 1014.56, 1338.86, 1456.26, 1506.41, 1554.63, 1649.14, and 3441.01 $cm^{-1}$, as seen in Figure-3. A prominent and strong peak was detected at around 3441.01 cm-1, indicating stretching vibrations of N–H and OH groups in

alcohol/phenol compounds such as flavonoids or terpenoids. The band at 2904 cm−1 corresponds to the aliphatic bending vibration of the C–H group (C-H), whereas the peak at 1649.14 $cm^{-1}$ is allocated to either the (C=C) group in alkenes or the carboxylic group. The aromatic bending vibration of the C-H group was assigned to smaller peaks at 1338.86, 1456.26, 1506.41, and 1554.63 $cm^{-1}$. Significant peaks at 422.41 $cm^{-1}$, 594.08 $cm^{-1}$, and 493.87 $cm^{-1}$ (Cu-O) suggest the synthesis of CuO NPs. As shown in Figure( 4).

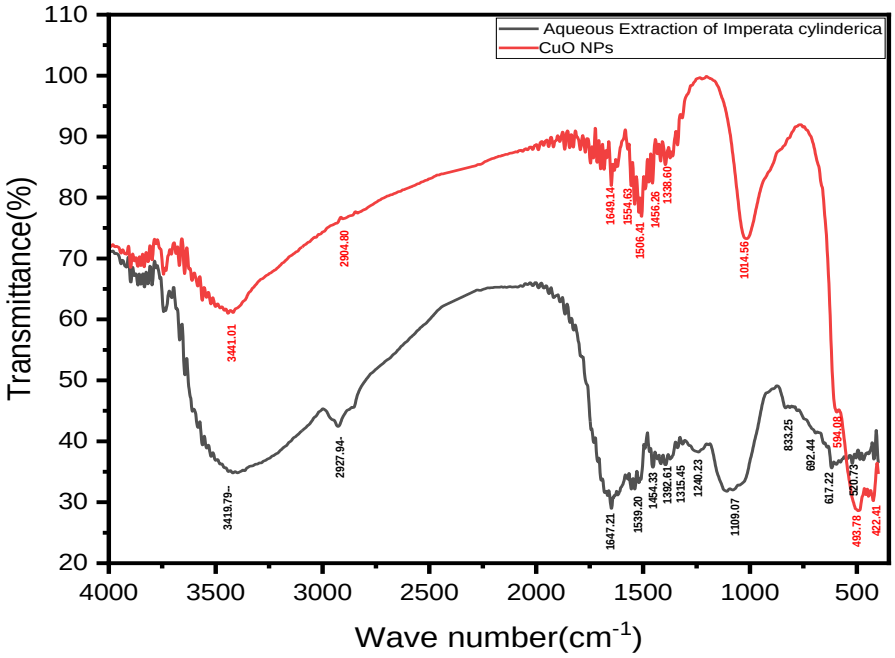


**Fig.4** *Fourier transform infrared spectroscopy (FTIR) of CuO nanoparticles and Aqueous extraction of Imperata Cylindric .*

### 3.1. 3. X-ray Diffraction (XRD)

The CuO nanostructured material's crystalline nature was investigated and analyzed using X-ray diffraction (XRD). The Debye-Scherrer formula was used to determine the average grain size of the material. equation (3)

$$D = k\lambda/\beta \cos \theta \qquad \text{eq.(3)}$$

where D represents the crystallite size in nanometers, k is Scherrer's constant with a value of 0.98, β is the full width at half maximum (FWHM), and Θ is the angle of diffraction are shown in table (2) [31]

The determined mean size of the nanoparticles is 10.9 nm. The PXRD diffraction graph (Figure 5) shows 11 distinct peaks corresponding to the monoclinic structure of CuO NPs at angles of (32.6°), (35.7°), (38.8°), (49.08°), (53.3°), (58.1°), (61.7°), (65.9°), (68.3°), (72.7°), and (75.6°). The peaks seen in the data correspond to the crystal planes (110), (-111), (200), (-202), (020), (202), (-113), (022), (220), (311), and (−222), respectively. The diffraction data obtained were found to be in good agreement with the standard JCPDS data card no. 00-041-0254 .[32]

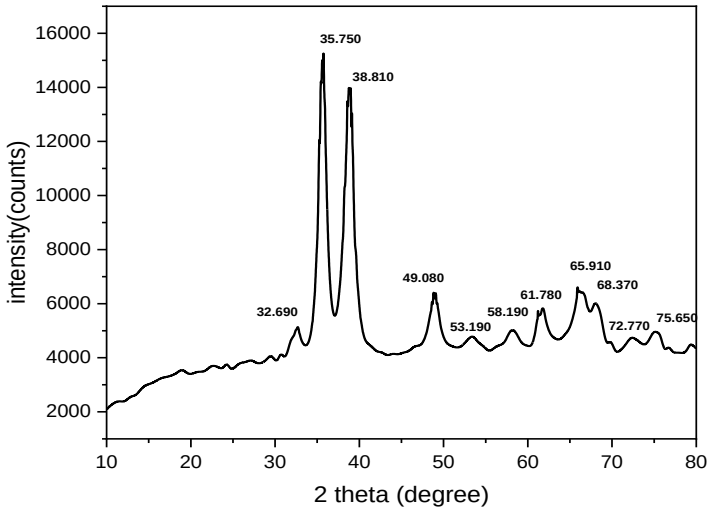


**Fig 5**. *XRD patterns of biosynthesized CuO nanoparticles*

**Table 2:** X-ray diffraction peak list of CuO nanoparticles

| Pos.[°2Th.] | Height [cts] | FWHM Left[°2Th.] | d-spacing [A°] | Rel. Int. [%] |
|---|---|---|---|---|
| 32.69 | 775.0908 | 0.1968 | 2.73775 | 7.44 |
| 35.75 | 10413.08 | 0.06 | 2.51544 | 100 |
| 38.81 | 9178.744 | 0.144 | 2.3204 | 88.15 |
| 49.08 | 1844.932 | 0.132 | 1.85444 | 17.72 |
| 53.39 | 372.0938 | 1.032 | 1.71392 | 3.57 |
| 61.21 | 1113.478 | 0.144 | 1.51296 | 10.69 |
| 61.78 | 1201.975 | 0.48 | 1.50225 | 11.54 |
| 65.91 | 1729.072 | 0.144 | 1.41677 | 16.6 |
| 68.37 | 949.1147 | 0.552 | 1.36547 | 2.88 |
| 72.77 | 299.731 | 0.984 | 1.30712 | 2.88 |
| 75.65 | 417.8657 | 0.672 | 1.25511 | 4.01 |

### 3.1. 4. Atomic Force Microscopy (AFM)

The Atomic Force Microscope (AFM) is a technique that provides high-resolution images used for studying the topography and morphology of CuO nanoparticles. The two and three-dimensional images, represented in figure (6-A), show that the CuO NPs in the 2D image appear spherical-like in shape with a uniform distribution in the scanned area (11.3 x 11.3 um). There is some aggregation, which results in the collection of more than three particles. The mean diameter of 315 particles in the desired area was determined using Mountains SPIP software and found to be 21.02nm, as shown in Figure (6-B). The surface roughness was determined by changes in the height and represented by parameters Sa (106.5nm) and Sq (129.4nm). These results show that the smooth surface is small-sized[33, 34].

(A)

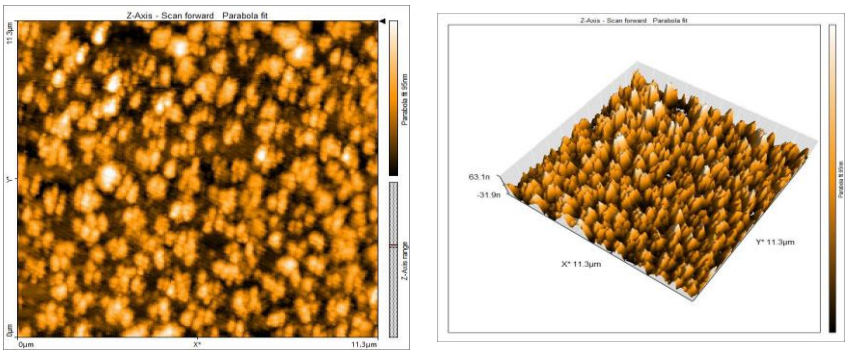


(B)

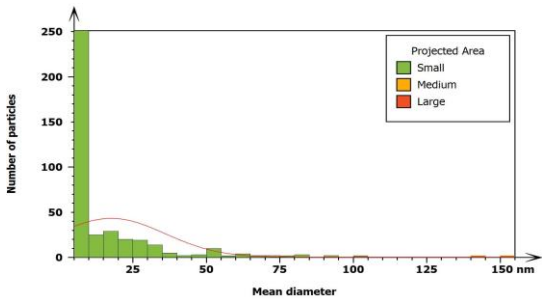


**Fig 6-A***: AFM image of green synthesized CuO NPs. (6-B) particles analysis with diameter range distribution*

### 3.1. 5. Field-emission scanning electron microscopy and energy dispersive X-ray spectroscopy (FESEM-EDX) analysis

Figure (7-A) displays the structural characteristics of CuO nanoparticles produced using the *Imperata cylindrica* extract. The results indicate that the copper nanoparticles have a spherical with size distribution ranging from 28.59 to 34.78 nm and relatively uniform shape, with aggregation occurring due to hydrogen bonding and electrostatic interactions between the bio-organic capping molecules of the plant extract.

In addition, Figure (7-B) displays the EDX analysis of significant signals for Cu(44.98%), confirming the synthesis of CuNPs, in addition to a minor proportion of carbon(4.73%) and silicon (7.27%) components attributed to the varying abundance and composition of capping agents of the extract. The presence of oxygen(43.02%), either through oxidation on the surface of the nanoparticles or through the polyphenol groups and other carbon-containing biomolecules in *Imperata cylindrica* leaves extract, contributed to the reduction and stabilization of CuNPs. [35]

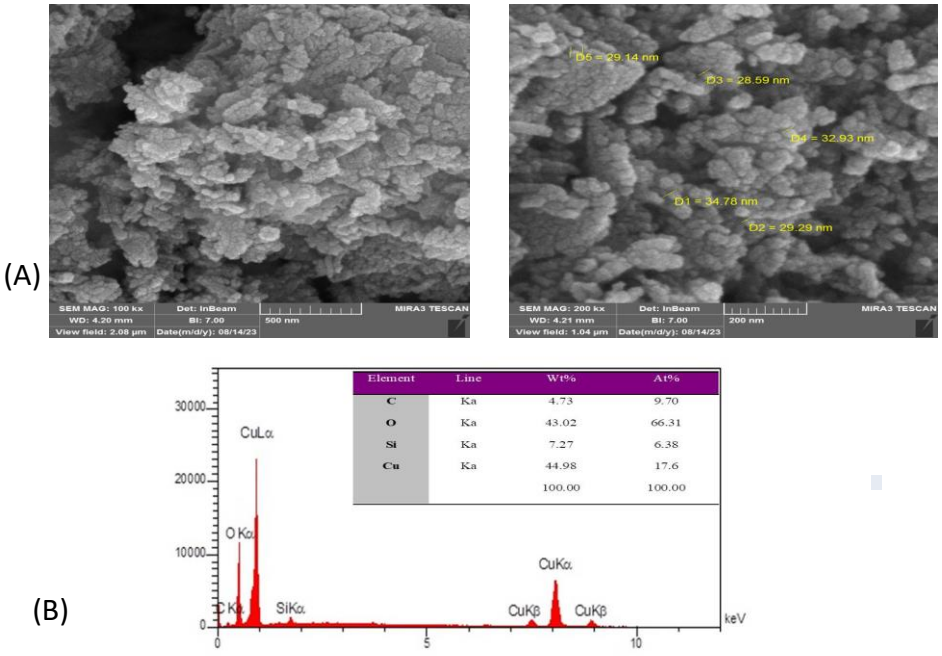


**Fig 7-A.** *shows the FESEM of CuO NPs synthesized by the Imperata cylindrica extract.* ***(7-B)*** *EDX analysis of CuO NPs*

### 3.1. 6. Zeta Potential analysis

The zeta potential analysis was conducted to elucidate the electrostatic charges and assess the stability of the nanoparticles. The zeta potential is a crucial characteristic that has a notable impact on the stability of colloidal dispersions. Particles with zeta potential values over ±30 mV often form stable dispersions[36].

Figure (8) demonstrates that the produced CuO NPs had a mean Zeta Potential value of +21.9 mV which quantifies the level of electrostatic repulsion between the particles that make up the colloid and formation stable form of nanoparticles.

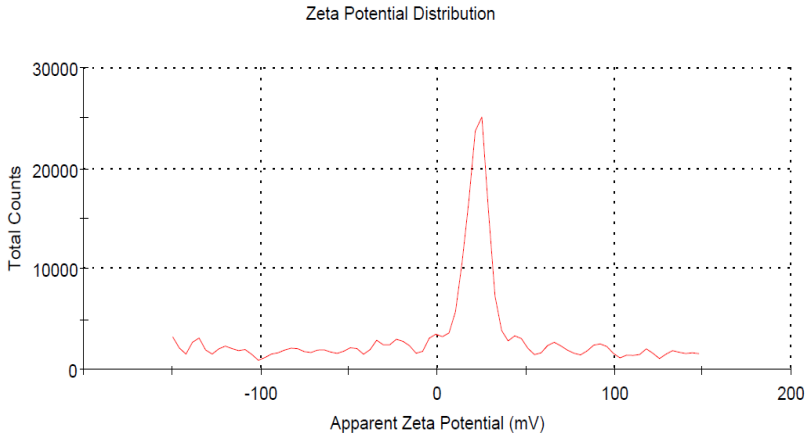


**Figure 8**. Zeta potential of CuO NPs

### 3.2. Cytotoxicity of CuO nanoparticles from I. cylindrica (cogon grass )

The MTT test was used to investigate the cytotoxic effect of *Imperata cylindrica*-mediated CuO NPs on the HCT-116 human colon cancer cell line. The cytotoxicity impact of CuO NPs on a human colon cancer cell line was assessed using doses of 10, 50, 100, 250, and 500 µg $mL^{-1}$, as seen in figure (9-A). The produced copper oxide nanoparticles have demonstrated a

substantial cytotoxic impact on a human colon cancer cell line, with an $IC_{50}$ value of 227.62 µg/ml. The cell viability percentage decreased when the concentration of nanoparticles increased. It reached 30.08% when the concentration of CuO NPs gradually increased to 250 µg $mL^{-1}$.

Conversely, the cell viability gradually increased to 32.84% when the concentration dose was 500 µg mL-1 in the human colon cancer cell line. The MTT findings of HFF cells demonstrated little toxicity of CuO NPs towards normal cells. According to the findings, when HFF normal cells were treated with a concentration of 500 µg/ml of CuO NPs for 24 hours, the cell viability was determined to be 83.6% (Figure 9-B). Consequently, the human colon cancer cell line exhibited much higher susceptibility to the biogenic CuO NPs than HFF normal cells. [37] Figure (10) displays the morphological alterations seen in both control and treated HCT-116 cells when exposed to varying concentrations of CuO NPs .

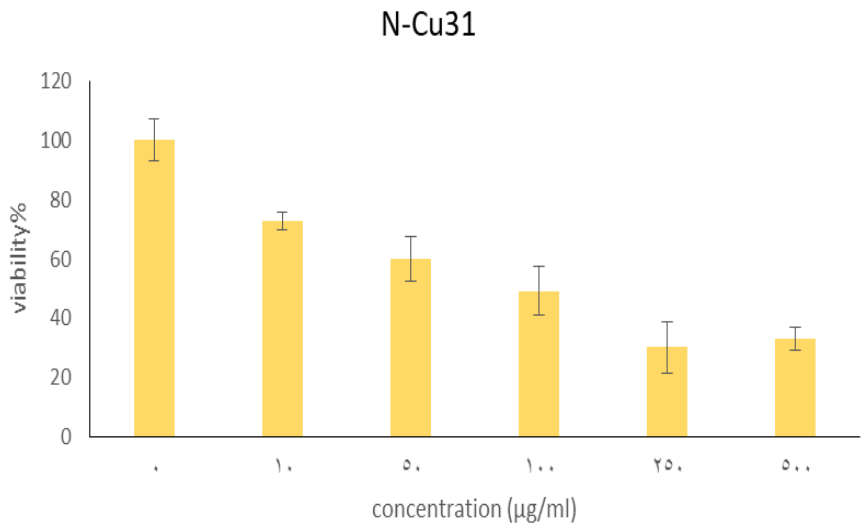


**Fig 9-A.** *MTT assay graph for anticancer activity of green synthesized CuO nanoparticles from Imperata cylindrica (cogon grass )*

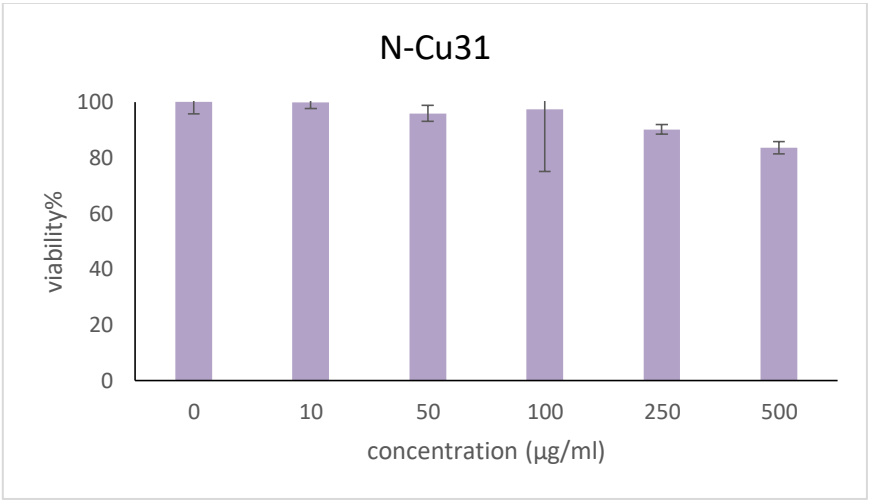


**Fig 9-B.** *MTT assay graph for anticancer activity of HFF cell lines viability*

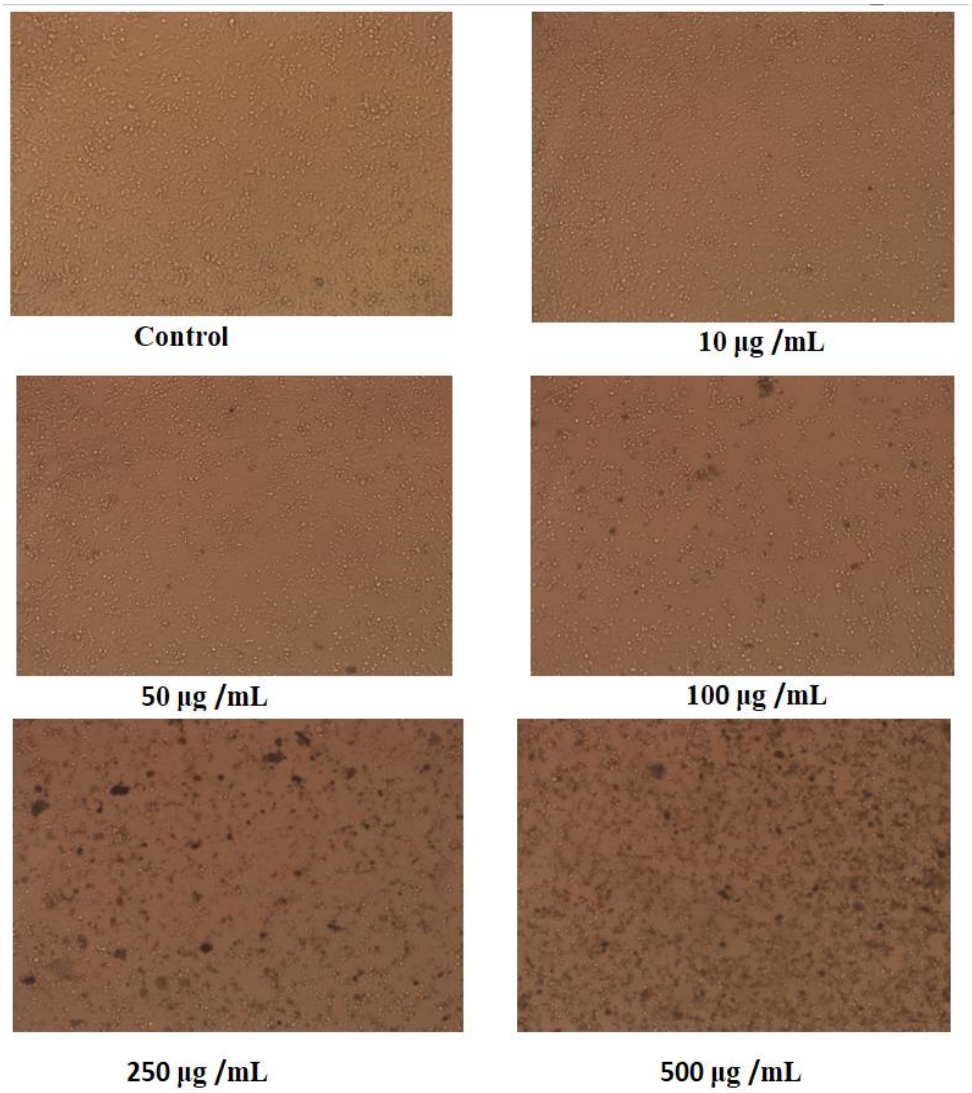


**Fig 10.** *Morphological changes in control and treated HCT-116 cells in different concentration of CuO NPs .*

### 3.3. Antibacterial Activity of CuO NPs

Numerous studies have indicated that copper oxide nanoparticles have significant antibacterial efficacy against pathogenic bacteria from Gram-positive and Gram-negative genera. [38-40]

Figure 11. The zone of inhibition of *Escherichia coli* and *Pseudomonas aeruginosa*, both Gram-negative bacteria, as well as *Staphylococcus aureus* and *Streptococcus*, both Gram-positive bacteria, was assessed in response to treatment with varied concentrations of produced CuO NPs.

The recorded diameters of the inhibition zones (in mm) surrounding the discs were compiled for various concentrations of Cu NPs, as presented in Table 3.

The width of the zone of inhibition provides insight into the extent of sensitivity of microorganisms. Copper nanoparticles exhibited significant antibacterial efficacy against all four species of bacteria at high concentrations. While the effectiveness of Cu NPs in low concentration (128 µg/ml) to eliminate microorganisms decreases, the inhibitory zone of microorganisms is either reduced in *Escherichia coli* or completely disappears in other kinds. figure(12).

Various recognized pathways exist for the antibacterial effects of metal nanoparticles. [41, 42]The predominant mechanism that has been identified involves the formation of reactive oxygen species (ROS). Copper nanoparticles (Cu NPs) significantly increase the cellular level of reactive oxygen species (ROS), affecting lipid peroxidation, protein oxidation, and DNA damage, ultimately leading to the death of microorganism cells. The ROS consist of reactive chemicals such as hydroxyl ions ($OH^-$), superoxide radicals ($O^{2-}$), and hydrogen peroxide ($H_2O_2$), which effectively eliminate microorganisms. [43, 44]

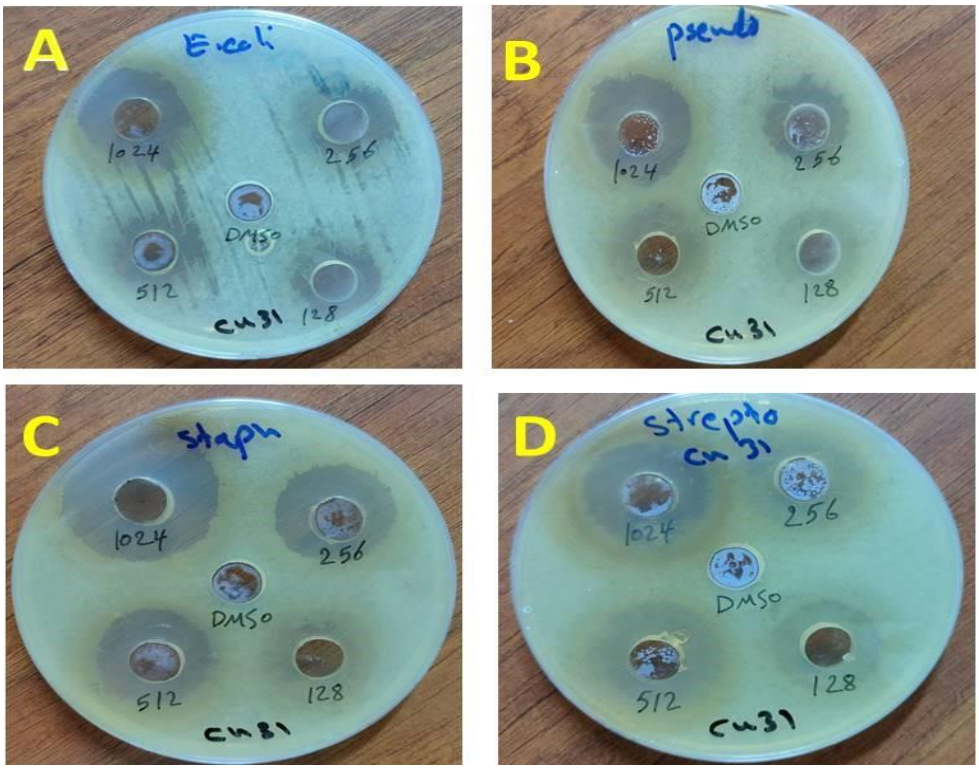


**Fig 11.** *Zone of inhibition of A- Escherichia coli B- Pseudomonas aeruginosa C-Staphylococci aureus D- Streptococcus in response to treatment with the synthesized CuO NPs in different concentration.*

**Table 3:** The results of antibacterial activity of CuO NPs in relation to NPs concentrations and bacterial isolates

| Concentrations of CuO NPs / Bacterial Isolates | 1024(µg/ml) | 512(µg/ml) | 256(µg/ml) | 128 (µg/ml) |
|---|---|---|---|---|
| ***Escherichia coli*** | 15 | 12 | 12 | 10 |
| ***Pseudomonas aeruginosa*** | 17 | 15 | 12 | Zero |
| ***Staphylococci aureus*** | 22 | 17 | 17 | Zero |
| ***Streptococcus*** | 20 | 17 | Zero | Zero |

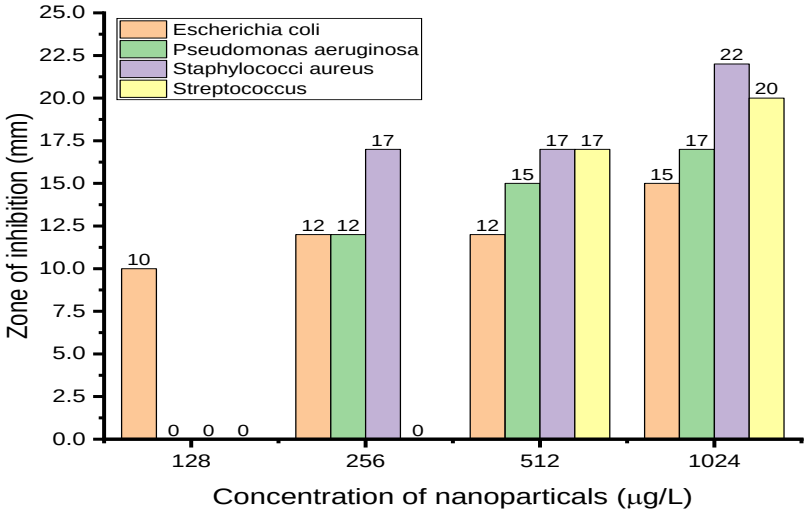


**Fig 12.** *graphical representation of zone of inhibition values at different concentration of Cu NPs*

## Conclusions

Imperata cylindrical is recognized as problematic and adversely affects agriculture and ecosystem health by outcompeting other plants; the study revealed that CuNPs were successfully synthesized and characterized by the green route. As confirmed FT-IR studies, the flavonoid and other phenolic compounds in *Imperata cylindrica* extract reduce $Cu^{2+}$ ions into Cu NPs.

It is used as an anticancer on human colon cancer cell lines (HCT-116) and as an antibacterial against gram-positive and gram-negative bacteria in different concentrations. The results showed that the nanoparticles' effect is directly proportional to the increase in concentration of CuNPs against Toxicology Evaluation.

## References

1. Sung, H., et al., *Global cancer statistics 2020: GLOBOCAN estimates of incidence and mortality worldwide for 36 cancers in 185 countries.* CA: a cancer journal for clinicians, 2021. **71**(3): p. 209-249.

2. Rasmussen, J.W., et al., *Zinc oxide nanoparticles for selective destruction of tumor cells and potential for drug delivery applications.* Expert opinion on drug delivery, 2010. **7**(9): p. 1063-1077.

3. Alavi, M. and R.S. Varma, *Phytosynthesis and modification of metal and metal oxide nanoparticles/nanocomposites for antibacterial and anticancer activities: Recent advances.* Sustainable Chemistry and Pharmacy, 2021. **21**: p. 100412.

4. Vinardell, M.P. and M. Mitjans, *Antitumor activities of metal oxide nanoparticles.* Nanomaterials, 2015. **5**(2): p. 1004-1021.

5. Halevas, E. and A. Pantazaki, *Copper nanoparticles as therapeutic anticancer agents.* Nanomed. Nanotechnol. J, 2018. **2**(1): p. 119-139.
6. Liao, G., et al., *Selenium nanoparticles (SeNPs) have potent antitumor activity against prostate cancer cells through the upregulation of miR-16.* World Journal of Surgical Oncology, 2020. **18**: p. 1-11.
7. Huang, H., et al., *Inspirations of cobalt oxide nanoparticle based anticancer therapeutics.* Pharmaceutics, 2021. **13**(10): p. 1599.
8. Alazzawi, A.A., A.N. Ghaloub, and L.A. Yaaqoob, *Investigating the Antioxidant and Apoptosis Inducing Effects of Biologically Synthesized Silver Nanoparticles Against Lymphoma Cells in Vitro.* Iraqi Journal of Science, 2023: p. 4390-4403.
9. Kajani, A.A., et al., *Gold nanoparticles as potent anticancer agent: green synthesis, characterization, and in vitro study.* RSC advances, 2016. **6**(68): p. 63973-63983.
10. Zhou, M., M. Tian, and C. Li, *Copper-based nanomaterials for cancer imaging and therapy.* Bioconjugate chemistry, 2016. **27**(5): p. 1188.1199-
11. Subashini, K., S. Prakash, and V. Sujatha, *Anticancer activity of copper oxide nanoparticles synthesized from brassia actinophylla flower extract.* Asian Journal of Chemistry, 2019. **31**: p. 1899-1904.
12. Manivannan, R., et al., *Green synthesis of Tecoma stans leaves-mediated copper oxide nanoparticles: Preparation, antioxidant, antimicrobial activities and in vitro MTT assay against MG-63 cell line.* Journal of Pharmacognosy and Phytochemistry, 2023. **12**(3): p. 195-201.
13. Bukhari, A., et al., *Green synthesis of metal and metal oxide nanoparticles using different plants' parts for antimicrobial activity and anticancer activity: a review article.* Coatings, 2021. **11**(11): p. 1374.
14. Minogue, P.J., B.V. Brodbeck, and J.H. Miller, *Biology and Control of Cogongrass (Imperata cylindrica) in Southern Forests: FR342/FR411, 3/2018.* EDIS, 2018. **2018**(2.(
15. Parkavi, V., et al., *Antibacterial activity of aerial parts of Imperata cylindrica (L) Beauv.* International Journal of Pharmaceutical Sciences and Drug Research, 2012. **4**(3): p. 209-212.
16. Krishnaiah, D., et al., *Studies on phytochemical constituents of six Malaysian medicinal plants.* Journal of medicinal plants research, 2009. **3**(2): p. 67-72.
17. Bonnia, N.N., et al. *Comparison study on biosynthesis of silver nanoparticles using fresh and hot air oven dried IMPERATA CYLINDRICA leaf*. in *IOP Conference Series: Materials Science and Engineering*. 2018. IOP Publishing.
18. Dong, F., et al., *Green synthesis of gold nanoparticles (AuNPs) as potential drug carrier for treatment and care of cardiac hypertrophy agents.* Journal of Cluster Science, 2022: p. 1-9.
19. Bonniaa, N.N., M.A. Ab Ranib, and A.A. Fairuzia, *Study on parameters optimization of silver nanoparticles biosynthesized using aqueous extract of Imperata cylindrica.* Desalination and Water Treatment, 2020. **174**: p. 186-195.
20. Nuradibah, M., et al. *Extraction of spear grass (Imperata Cylindrica) as pro-oxidant in polymer blends*. in *MATEC Web of Conferences*. 2018. EDP Sciences.
21. Benhammada, A. and D. Trache, *Green synthesis of CuO nanoparticles using Malva sylvestris leaf extract with different copper precursors and their effect on nitrocellulose thermal behavior.* Journal of Thermal Analysis and Calorimetry, 2022. **147**: p. 1-16.

22. Qasem, M., R. El Kurdi, and D. Patra, *Green synthesis of curcumin conjugated CuO nanoparticles for catalytic reduction of methylene blue.* ChemistrySelect, 2020. **5**(5): p. 1694-1704.
23. Peter, A., *Synthesis of CuO Nanomaterials with Controllable Morphologies by Changing the pH.* Proceedings of the Yukthi, 2021.
24. Khit, S.A., E.T. Kareem, and I.M. Shaheed, *Eco-Friendly Synthesized of CuO Nanoparticles Using Anchusa strigosa L. Flowers and Study its Adsorption Activity.* Baghdad Science Journal, 2023.
25. Atiya, M.A., A.K .Hassan, and F.Q. Kadhim, *Green Synthesis of Copper Nanoparticles Using Tea Leaves Extract to Remove Ciprofloxacin (CIP) from Aqueous Media.* Iraqi Journal of Science, 2021: p. 2832-2854.
26. Kukia, N.R., et al., *Bio-effects of TiO2 nanoparticles on human colorectal cancer and umbilical vein endothelial cell lines.* Asian Pacific journal of cancer prevention: APJCP, 2018. **19**(10): p. 2821.
27. Prabhu, Y., et al., *A facile biosynthesis of copper nanoparticles: A micro-structural and antibacterial activity investigation.* Journal of Saudi Chemical Society, 2017. **21**(2): p. 180-185.
28. Arun, K., et al., *Surfactant free hydrothermal synthesis of copper oxide nanoparticles.* Am. J. Mater. Sci, 2015. **5**(3A): p. 36-38.
29. Jabar, Z.S. and M.H. Hassouni, *Preparation and Characterization of Copper Oxide Nanoparticles by Precipitation Method for Photonics and Optoelectronics.* IRAQI JOURNAL OF APPLIED PHYSICS, 2023. **19**: p. 37-42.
30. Siddiqui, H., M. Qureshi, and F.Z. Haque, *Valuation of copper oxide (CuO) nanoflakes for its suitability as an absorbing material in solar cells fabrication.* Optik, 2016. **127**(8): p. 3713-3717.
31. Abdulredha, S.T. and N.A. Abdulrahman, *Cu-ZnO Nanostructures Synthesis and Characterization.* Iraqi Journal of Science, 2021: p. 708-717.
32. Aroob ,S., et al., *Green Synthesis and Photocatalytic Dye Degradation Activity of CuO Nanoparticles.* Catalysts, 2023. **13**(3): p. 502.
33. Shanan, Z.J., S.M. Hadi, and S.K. Shanshool, *Structural analysis of chemical and green synthesis of CuO nanoparticles and their effect on biofilm formation.* Baghdad Science Journal, 2018. **15**(2): p. 0211-0211.
34. Taha, J.H., N.K. Abbas, and A.A. Al-Attraqchi, *Green Synthesis and Evaluation of Copper Oxide Nanoparticles using Fig Leaves and their Antifungal and Antibacterial Activities.* Int. J. Drug Delivery Technol, 2020. **10**: p. 378-382.
35. Ahmed, A., et al., *Plant mediated synthesis of copper nanoparticles by using Camelia sinensis leaves extract and their applications in dye degradation.* Ferroelectrics, 2019. **549**(1): p. 61-6.9
36. Sankhla, A., et al., *Biosynthesis and characterization of cadmium sulfide nanoparticles–an emphasis of zeta potential behavior due to capping.* Materials Chemistry and Physics, 2016. **170**: p. 44-51.
37. Dolati, M., et al., *Biogenic copper oxide nanoparticles from Bacillus coagulans induced reactive oxygen species generation and apoptotic and anti-metastatic activities in breast cancer cells.* Scientific Reports, 2023. **13**(1): p. 3256.
38. Abed, S.M., et al., *Antibacterial Activity of Green Synthesized Copper Oxide Nanoparticles.* Iraqi Journal of Science, 2021: p. 3372-3383.

39. Shanmugapriya, J., et al., *Green synthesis of copper nanoparticles using Withania somnifera and its antioxidant and antibacterial activity.* Journal of Nanomaterials, 2022. 2022.
40. Naradala, J., et al., *Antibacterial activity of copper nanoparticles synthesized by Bambusa arundinacea leaves extract.* Biointerface Res. Appl. Chem, 2021. **12**: p. 1230-1236.
41. Erci, F., et al., *Synthesis of biologically active copper oxide nanoparticles as promising novel antibacterial-antibiofilm agents.* Preparative Biochemistry & Biotechnology, 2020. **50**(6): p. 538-548.
42. Wu, S., et al., *Green synthesis of copper nanoparticles using Cissus vitiginea and its antioxidant and antibacterial activity against urinary tract infection pathogens.* Artificial Cells, Nanomedicine, and Biotechnology, 2020. **48**(1): p. 1153-1158.
43. Mali, S.C., et al., *Green synthesis of copper nanoparticles using Celastrus paniculatus Willd. leaf extract and their photocatalytic and antifungal properties.* Biotechnology Reports, 2020. **27**: p. e00518.
44. Rand, M., *SYNERGISTIC EFFECT OF COPPER OXIDE NANOPARTICLES FOR ENHANCING ANTIMICROBIAL ACTIVITY AGAINST K. PNEUMONIAE AND S. AUREUS.* IRAQI JOURNAL OF AGRICULTURAL SCIENCES, 202 :(1)55 .4p. 353-360.

IRAQI Academic Scientific Journals
Samarra Journal of Pure and Applied Science
SJPAS
مجلة سامراء للعلوم البحتة والتطبيقية
www.sjpas.com
p ISSN: 2663-7405
e ISSN: 2789-6838

# تصنيع جسيمات أكاسيد النحاس النانوية الخضراء المنتجة من نبات الحلفا وتقييم فعاليتها في تثبيط نمو خلايا (HCT-116) والنشاط المضاد للبكتيريا

**محمد محمود مسعود*، وضاح ناجي جاسم السعيدي**

قسم الكيمياء، كلية العلوم، جامعة بغداد، العراق

**معلومات البحث:**

تأريخ الاستلام: 2024/03/10
تاريخ التعديل: 2024/04/20
تأريخ القبــول: 2024/05/28
تاريخ الـنشر: 2025/03/30

**الكلمات المفتاحية:**

اكاسيد النحاس النانوية، نبات الحلفا، مضادات السرطان، مضادات البكتيريا

**معلومات المؤلف**

الايميل:
Mohammed.mahmoud1105d@sc.uobaghdad.edu.iq
الموبايل:9647736914970+

**الخلاصة:**

تبحث الدراسة الحالية لدراسة مضادات السرطان ومضادات البكتيريا مختبريًا لأكاسيد النحاس النانوية (CuO NPs) التي تم تصنيعها من نبات الحلفا *Imperata cylindrical* باستخدام اختبار MTT (3-(4,5-dimethylthiazol-2-yl)-2,5-diphenyl-2H-tetrazolium bromide). وطريقة الانتشار القرصي تم تشخيص الجسيمات النانوية المصنعة باستخدام تقنيات تحليلية مختلفة مثل الأشعة فوق البنفسجية- المرئية، و الأشعة تحت الحمراء، وتحليلات الأشعة السينية المشتتة للطاقة، والمجهر الالكتروني الماسح، ومجهر القوى الذرية، وتحليل إمكانات زيتا. تمت دراسة كفاءة CuO NPs على خطوط خلايا سرطان القولون البشرية (HCT-116) وخلايا (HFF) كخطوط خلايا طبيعية. تم اختيار تركيزات مختلفة من جسيمات أكسيد النحاس النانوية (10، 50، 100، 500،250) ميكروغرام / مل عند 24 ساعة. أظهرت النتائج أن تأثير الجسيمات النانوية يعتمد على التركيز. ومع زيادة تركيز الجسيمات النانوية تنخفض نسبة صلاحية الخلية. وجد أن تركيز جزيئات أكسيد النحاس النانوية عند 250 ميكروغرام/مل أعطى نسبة حيوية الخلية (30.08%) بعد 24 ساعة. كما أظهرت الجسيمات النانوية تأثيرات مضادة للبكتيريا ضد البكتيريا الموجبة والسالبة الغرام وبتراكيز مختلفة. بتركيز 1024 (ميكروجرام/مل)، أظهرت CuO NPs تأثيرًا قويًا مضادًا للبكتيريا ضد جميع أنواع البكتيريا الأربعة.